Semiconductor Physics, Quantum Electronics & Optoelectronics, 2024. V. 27, No 2. P. 176-183.

Semiconductor physics

Phase transition and comparative study of $Cu_xCd_{1-x}S$ (x = 0.8, 0.6, 0.4, and 0.2) nanoparticle system

M.M. Rose[1,*], R.S. Christy[1], T.A. Benitta[1], J.T.T. Kumaran[3]

[1]*Mar Ephraem College* of *Engineering and Technologies, Elavuvilai, Tamilnadu, India*
[2]*Department of Physics and Research Centre, Nesamony Memorial Christian College, Marthandam, Affiliated to Manonmaniam Sundaranar University, Abishekapatti, Tirunelveli, Tamilnadu, India*
[3]*Department of Physics and Research Centre, Malankara Catholic College Mariagiri*
[*]*Corresponding author e-mail: molyrengith@gmail.com*

Abstract. Microwave-assisted chemical precipitation was used to prepare $Cu_xCd_{1-x}S$ (x = 0.8, 0.6, 0.4, and 0.2) nanoparticles mixture. The crystal structure, size, and surface morphology of the as-synthesized nanoparticles were studied using X-ray diffraction and SEM. Presence of copper, cadmium, and sulphur in proper ratios in the samples was confirmed by energy-dispersed X-ray analysis. DC electrical resistance measurements of all the samples in the temperature range of 300…500 K showed phase transition above a certain temperature.

Keywords: nanoparticles, chemical precipitation, phase transition, band gap energy, electrical resistance.

https://doi.org/10.15407/spqeo27.02.176
PACS 61.05.cp, 64.70.Nd, 68.37.Hk

Manuscript received 11.01.24; revised version received 26.03.24; accepted for publication 19.06.24; published online 21.06.24.

1. Introduction

Copper sulphide (CuS) is an important semiconductor material, which has a wurtzite crystal structure and a direct band gap of 2.5 eV [1, 2]. Copper sulphide nanoparticles (NPs) are required for fabricating solar cell components [3], fluorescent devices [4], photocatalysts [5], thermoelectric [6] and photoacoustic devices [7], medicinal materials [8], and photothermal switches [9].

Cadmium sulphide (CdS) is another important semiconductor with a direct band gap of 2.42 eV [10] that finds applications in solar cells, diodes, photo-catalysts, field effect transistors, and electrically powered lasers [11–15]. Nanoparticles of $Cu_xCd_{1-x}S$ (x = 0.8, 0.6, 0.4, and 0.2) solid solutions may be obtained that combine properties of both copper sulphide and cadmium sulphide NPs.

S.L. Prokopenko and G.M. Gunja obtained CuS/CdS heterostructures and investigated their electrical properties [16]. Metal cations and sulphide anions underwent layer-by-layer interactions to create composite sensitizers that contained CuS and CdS quantum dots [17]. Xiande Yang and Guangwen Lu used a hydrothermal method to create CdS/CuS composites and studied their optical properties [18]. CuS microflower – 2D graphene hybrids (CdS/CuS-MF/G) decorated by CdS nanoparticles were created by Z.G. Li and B. Zeng [19].

In this work, we synthesized $Cu_xCd_{1-x}S$ (x = 0.8, 0.6, 0.4, and 0.2) NPs by a microwave-assisted chemical precipitation method and investigated phase transitions in them using DC electrical measurements. Optical properties of the samples were studied and compared by analyzing UV absorption and PL emission spectra.

2. Experimental details

2.1. Synthesis of $Cu_xCd_{1-x}S$ (x = 0.8, 0.6, 0.4, and 0.2) NPs by microwave assisted chemical precipitation method

$Cu_xCd_{1-x}S$ (x = 0.8, 0.6, 0.4, and 0.2) NPs were prepared using a 1:2 molar ratio of copper acetate, cadmium acetate, and sodium sulphide. Copper acetate and cadmium acetate were mixed together after being separately dissolved in 40 ml of distilled water. A sodium sulphide solution obtained by dissolving 6.14 g sodium sulphide in 40 ml of distilled water was dropped to the above solution during 3 hours at intense stirring and then left undisturbed for one day. As precipitation was completed, the precipitates were separated, washed several times with deionized water, and stored in a microwave oven. The solution was then microwave-irradiated for 20 min at 800 W. The resulting NPs were cooled down to the ambient temperature. Finally, the NPs were annealed at 100 °C for 3 hours to synthesize pure $Cu_xCd_{1-x}S$ (x = 0.8, 0.6, 0.4, and 0.2) NPs. Table 1 shows

Table 1. Amounts of precursor materials to be dissolved in 80 ml of distilled water for synthesizing $Cu_xCd_{1-x}S$ (x = 0.8, 0.6, 0.4, and 0.2) NPs.

Sample number	Expected composition	Copper acetate (g)	Cadmium acetate (g)
1	$Cu_{0.8}Cd_{0.2}S$	6.38	2.13
2	$Cu_{0.6}Cd_{0.4}S$	4.79	4.26
3	$Cu_{0.4}Cd_{0.6}S$	3.19	6.39
4	$Cu_{0.2}Cd_{0.8}S$	1.59	8.52

the amounts of the precursor materials to be dissolved in 80 ml of distilled water to synthesize $Cu_xCd_{1-x}S$ (x = 0.8, 0.6, 0.4, and 0.2) NPs.

The collected $Cu_xCd_{1-x}S$ (x = 0.8, 0.6, 0.4, 0.2) NPs were used for characterization. The resistance measurements were carried out on the pellet shaped samples.

2.2. Instrumentation

X-ray diffraction (XRD) patterns of the synthesized nanoparticles were captured in the 2θ range of 10°…80° using a powder X-ray diffractometer with a CuK_α radiation source (λ = 1.54 Å). A TESCAN VEGA3 SBH scanning electron microscope was used to examine surface morphology of the materials. An energy dispersive X-ray analysis (EDAX) apparatus connected to a scanning electron microscope was used to analyze the element compositions. A UV-visible range spectrometer was used to capture optical absorption spectra of the synthesized NPs in the wavelength range of 200 to 900 nm. Photoluminescence spectra in the wavelength range of 300 to 650 nm were measured using a Varian Cary Eclipse photoluminescence spectrophotometer. NPs pellets were fabricated by applying a pressure of 10 tonnes/cm^2. The resistance of the fabricated pellets was measured by a four-probe technique.

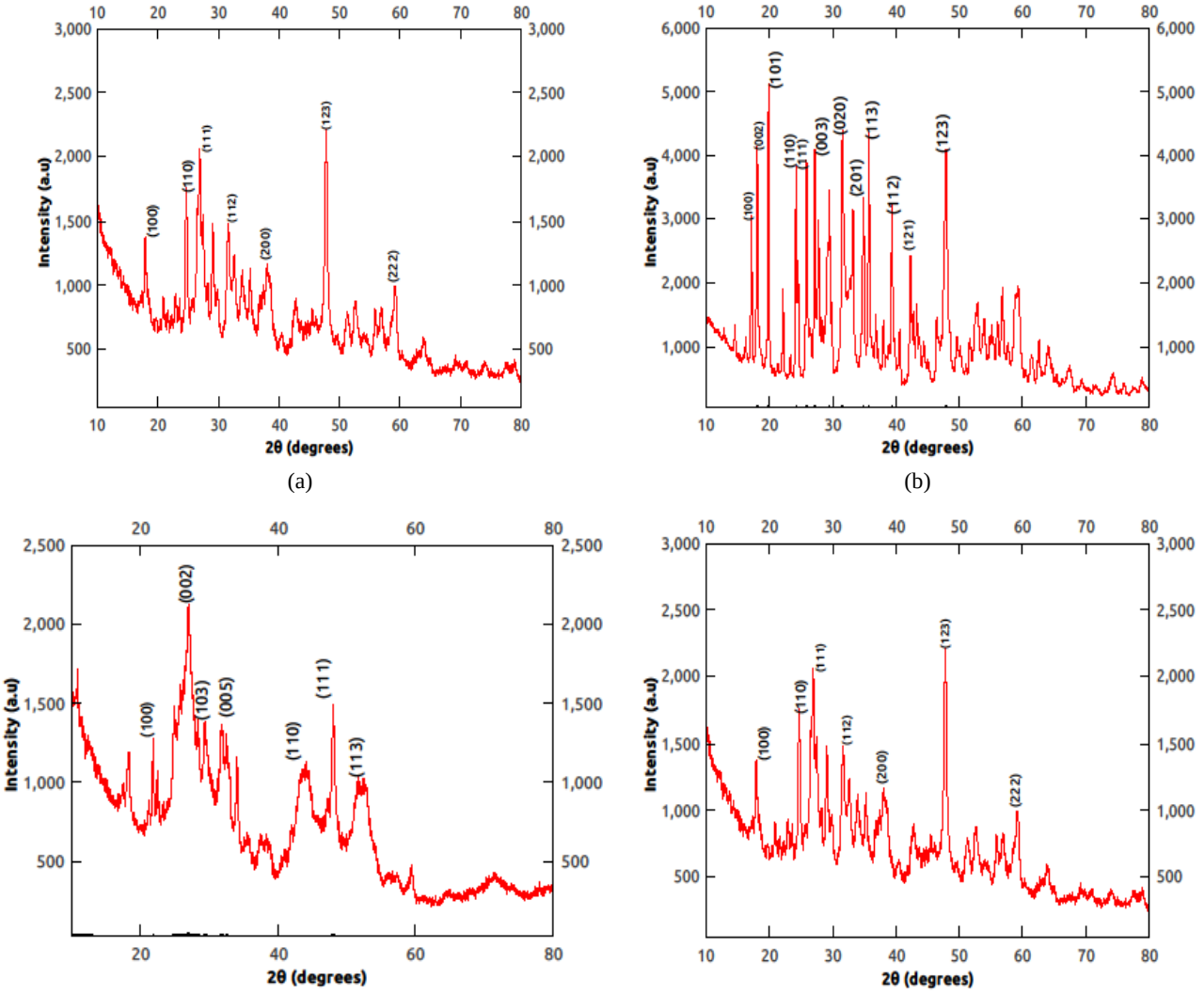

Fig. 1. Indexed XRD patterns of $Cu_xCd_{1-x}S$ (x = 0.8, 0.6, 0.4, 0.2) NPs: $Cu_{0.8}Cd_{0.2}S$ (a), $Cu_{0.6}Cd_{0.4}S$ (b), $Cu_{0.4}Cd_{0.6}S$ (c), $Cu_{0.2}Cd_{0.8}S$ (d).

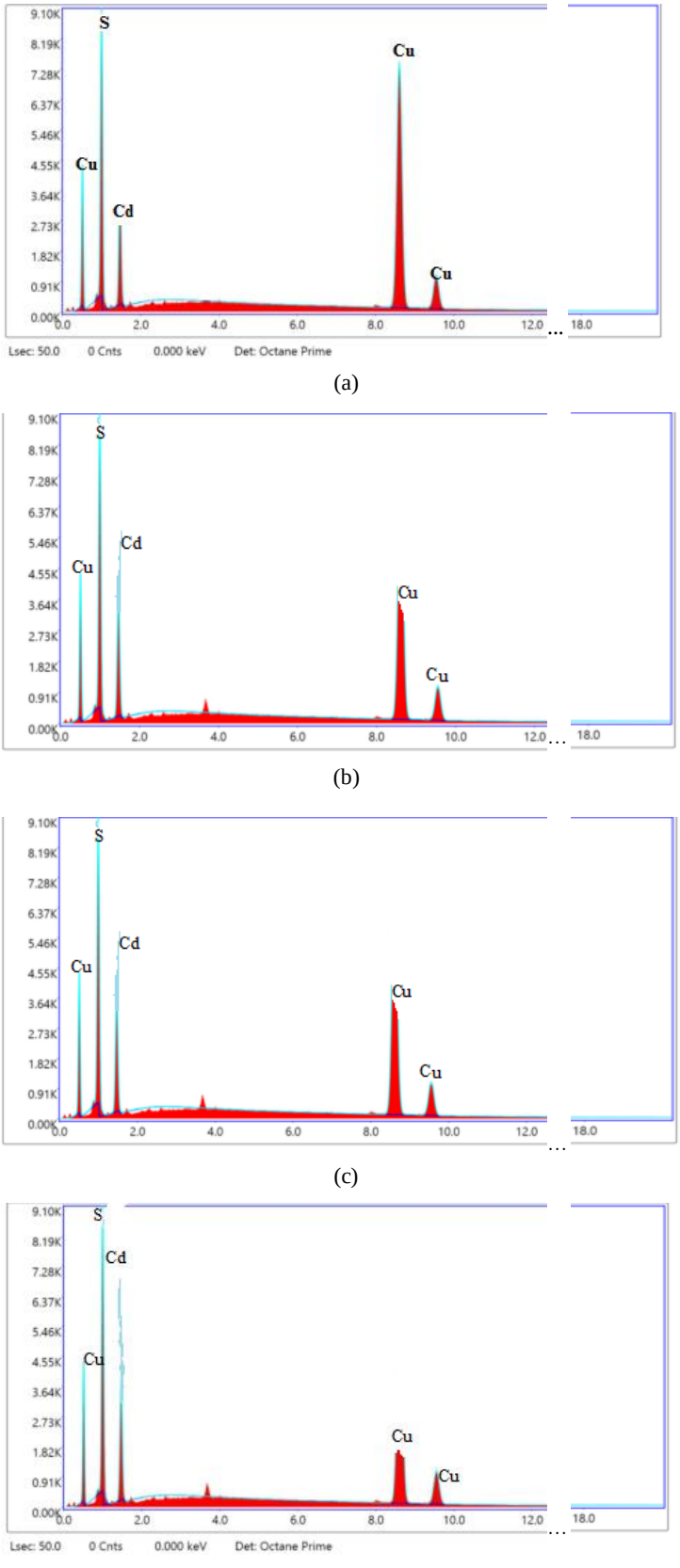

(a) (b) (c) (d)

Fig. 2. EDAX images of $Cu_xCd_{1-x}S$ (x = 0.8, 0.6, 0.4, and 0.2) NPs: $Cu_{0.8}Cd_{0.2}S$ (a), $Cu_{0.6}Cd_{0.4}S$ (b), $Cu_{0.4}Cd_{0.6}S$ (c), and $Cu_{0.2}Cd_{0.8}S$ (d).

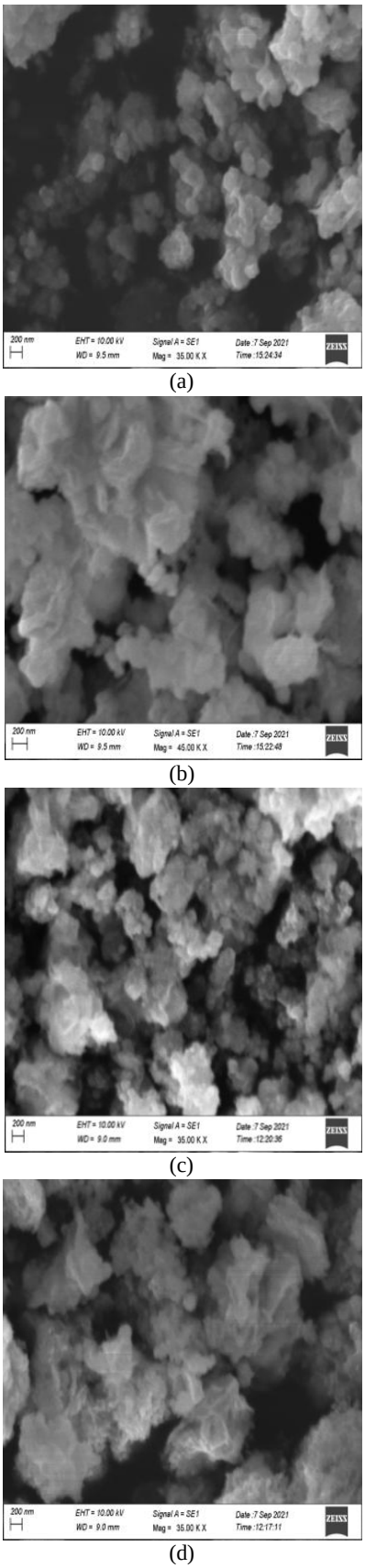

(a) (b) (c) (d)

Fig. 3. SEM images of $Cu_xCd_{1-x}S$ (x = 0.8, 0.6, 0.4, 0.2) NPs: $Cu_{0.8}Cd_{0.2}S$ (a), $Cu_{0.6}Cd_{0.4}S$ (b), $Cu_{0.4}Cd_{0.6}S$ (c), $Cu_{0.2}Cd_{0.8}S$ (d).

3. Results and discussion

3.1. Structural studies of $Cu_xCd_{1-x}S$ (x = 0.8, 0.6, 0.4, and 0.2) NPs

The indexed XRD patterns of the $Cu_xCd_{1-x}S$ (x = 0.8, 0.6, 0.4, and 0.2) NPs are shown in Fig. 1. The NP compositions were confirmed by the EDAX images shown in Fig. 2. SEM images of all the samples (Fig. 3) confirm the presence of nanostructures. Table 2 summarizes the synthesized samples compositions, their structures at room temperature, lattice parameters, and particle sizes.

Structural studies of the $Cu_xCd_{1-x}S$ (x = 0.8, 0.6, 0.4, and 0.2) NPs have revealed that the solid solutions may have the structure of any of their components at room or higher temperatures [20]. By replacing 20% of Cu by Cd in the $Cu_{0.6}Cd_{0.4}S$ composition, the nanoparticle size can be reduced to half keeping the structure the same. Further replacing Cu by Cd changes the structure to hexagonal.

Table 2. Compositions, structures at room temperature, lattice parameters and particle sizes of the synthesized samples.

Sample number	Composition	Structure at room temperature	Lattice parameters	Particle size, nm
	CuS (reported) [20]	Hexagonal	a = 3.77 Å, c = 16.42 Å	
1	$Cu_{0.8}Cd_{0.2}S$	Tetragonal	$a = b$ = 4.85 Å, c = 7.17 Å	31
2	$Cu_{0.6}Cd_{0.4}S$	Tetragonal	$a = b$ = 5.13 Å, c = 9.75 Å	34
3	$Cu_{0.4}Cd_{0.6}S$	Tetragonal	$a = b$ = 4.91 Å, c = 8.42 Å	16
4	$Cu_{0.2}Cd_{0.8}S$	Hexagonal	$a = b$ = 4.82 Å, c = 12.83 Å	17
	CdS (reported) [21]	Hexagonal	$a = b$ = 4.16 Å, c = 6.76 Å	

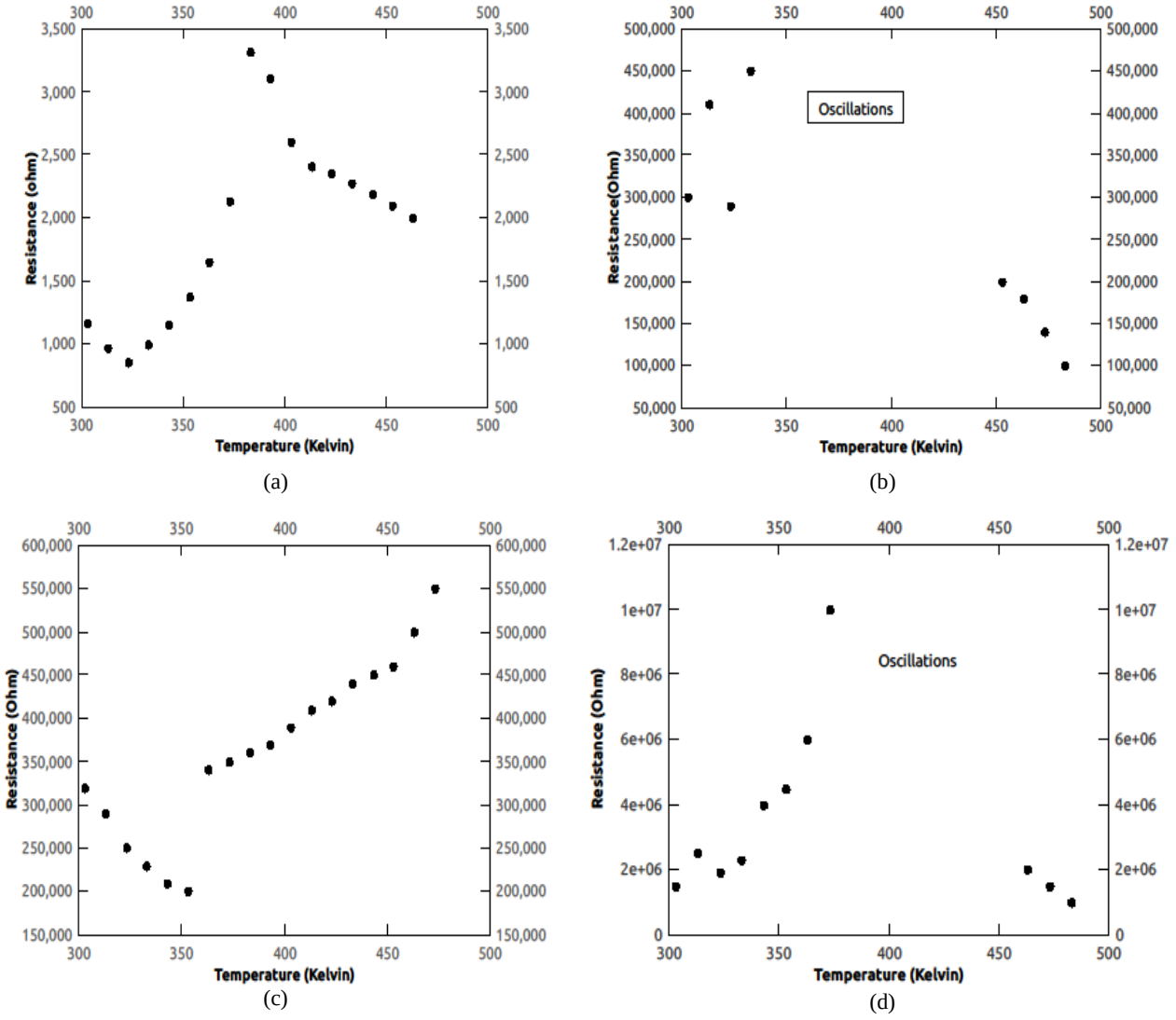

Fig. 4. Indexed XRD patterns of $Cu_xCd_{1-x}S$ (x = 0.8, 0.6, 0.4, 0.2) NPs: $Cu_{0.8}Cd_{0.2}S$ (a), $Cu_{0.6}Cd_{0.4}S$ (b), $Cu_{0.4}Cd_{0.6}S$ (c), $Cu_{0.2}Cd_{0.8}S$ (d).

3.2. Electrical studies of $Cu_xCd_{1-x}S$ (x = 0.8, 0.6, 0.4, and 0.2) NPs

Fig. 4 shows temperature dependences of the resistance of the $Cu_xCd_{1-x}S$ (x = 0.8, 0.6, 0.4, and 0.2) NPs synthesized by the microwave assisted chemical precipitation method. Since CdS and CuS NPs show a phase transition above a certain temperature in the measurement range [21, 22], a discontinuity of all the curves above this temperature is observed indicating the change of the sample electrical properties [23].

Temperature dependence of the resistance of the $Cu_{0.8}Cd_{0.2}S$ NPs is shown in Fig. 4a. This curve is similar to the one for CuS NPs synthesized by solvothermal method [22], the difference being the shift of the transition temperature to the very low value (330 K).

Fig. 4b shows temperature dependence of the resistance of $Cu_{0.6}Cd_{0.4}S$ NPs. It can be seen from this figure that the resistance slightly fluctuates between 300 and 340 K. Resistance measurements become challenging between 350 and 440 K due to strong fluctuations evidencing a close to the phase transition region [24]. The resistance smoothly decreases with temperature above 440 K showing the behaviour of a semiconductor. Hence, $Cu_{0.6}Cd_{0.4}S$ may be used as a good semi-conducting material at temperatures exceeding 400 K.

It can be seen from Fig. 4c that $Cu_{0.4}Cd_{0.6}S$ NPs act as a semiconductor even at room temperature, which distinguishes this material from the $Cu_{0.6}Cd_{0.4}S$ NPs.

Fig. 4d presents temperature dependence of the resistance of the $Cu_{0.2}Cd_{0.8}S$ NPs. A steep rise to very high temperature and followed by oscillations in four probe resistance measurement and switch back to resistance at room temperature and above 460 K it may behave as a semiconductor.

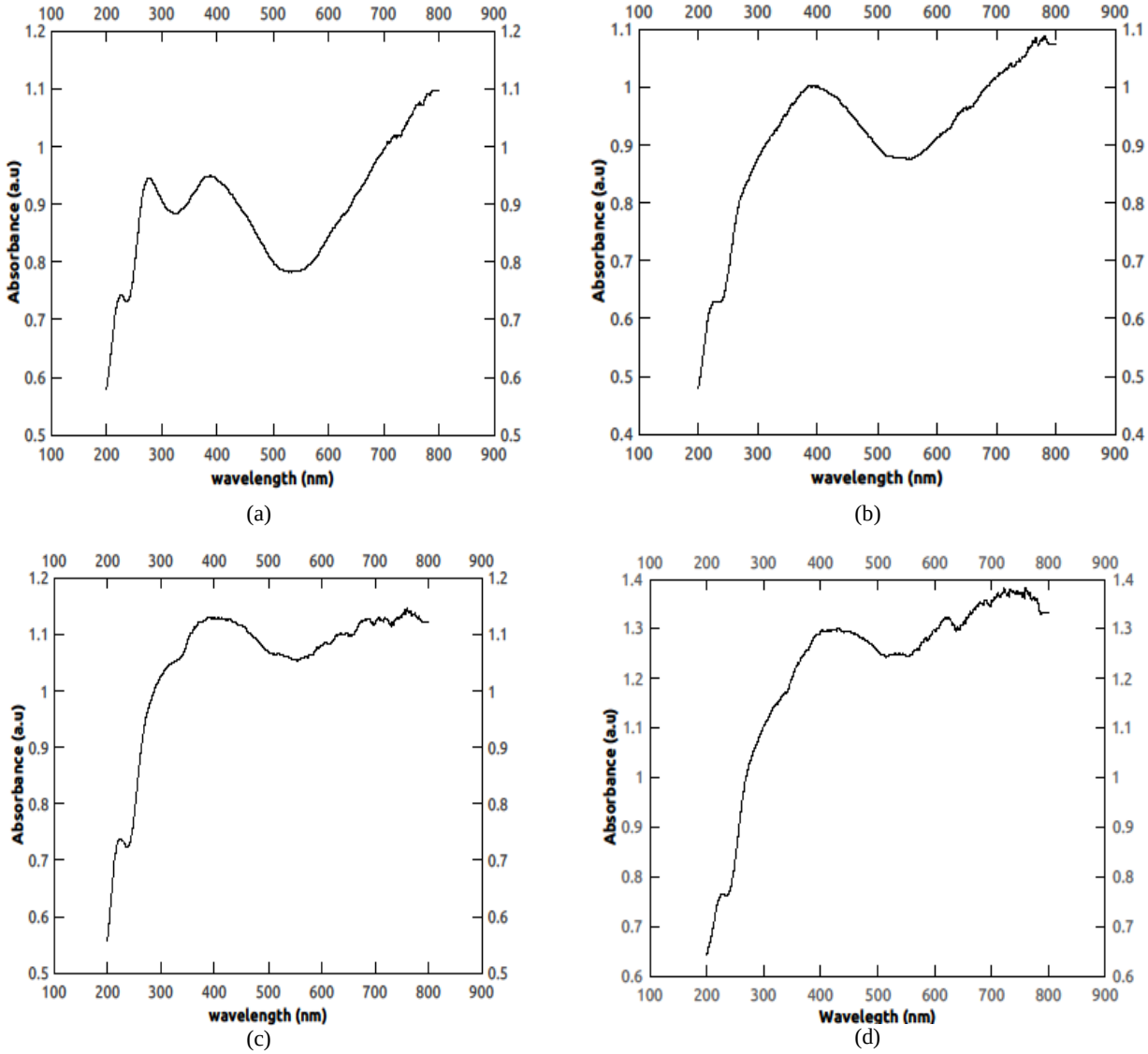

Fig. 5. Optical absorption spectra of $Cu_xCd_{1-x}S$ (x = 0.8, 0.6, 0.4, and 0.2) NPs: $Cu_{0.8}Cd_{0.2}S$ (a), $Cu_{0.6}Cd_{0.4}S$ (b), $Cu_{0.4}Cd_{0.6}S$ (c), and $Cu_{0.2}Cd_{0.8}S$ (d).

Table 3. Order of resistance at room temperature, behaviour at room temperature and possible transition temperatures of $Cu_xCd_{1-x}S$ (x = 0.8, 0.6, 0.4, and 0.2) NPs.

Samples	Order of resistance at room temperature	Behaviour of the sample at room temperature	Possible transition temperatures, K
$Cu_{0.8}Cd_{0.2}S$	10^3 Ohm	semiconductor	>330
$Cu_{0.6}Cd_{0.4}S$	10^5 Ohm	small oscillation	>440
$Cu_{0.4}Cd_{0.6}S$	10^5 Ohm	semiconductor	>360
$Cu_{0.2}Cd_{0.8}S$	10^5 Ohm	small oscillation	>460

The order of the resistance at room temperature, the behaviour at room temperature and possible transition temperatures of the $Cu_xCd_{1-x}S$ (x = 0.8, 0.6, 0.4, and 0.2) NPs are summarized in Table 3.

As can be seen from Table 3, replacing of 20% of Cu by Cd in the $Cu_{0.8}Cd_{0.2}S$ NPs makes the resistance at room temperature change from ~10^3 to ~10^5 Ohm.

3.3. Optical studies of $Cu_xCd_{1-x}S$ (x = 0.8, 0.6, 0.4, and 0.2) NPs

3.3.1. UV studies

Fig. 5a presents the optical absorption spectrum of the $Cu_{0.8}Cd_{0.2}S$ NPs. As can be seen from this figure, there is an absorption band between 200 and 500 nm with sharp peaks at 280 and 400 nm and a dip between them. The absorption edge at 500 nm is the one observed for pure CuS NPs [25, 26]. One can see one more absorption edge above 800 nm, which is also characteristic for pure CuS NPs [27]. The peak at 280 nm identifies $Cu_{0.8}Cd_{0.2}S$ NPs. It disappears when 20% of Cd is replaced by Cu (Fig. 5b). For the samples with higher Cd content, the absorption band peaked at 400 nm merges with the absorption band having an edge above the measurement range. As a result, a single band with one edge below 40 nm and the other edge beyond the measurement range forms (Figs. 5c and 5d). Hence, the samples under consi-deration may be used as optical filters to filter out all the wavelengths above 300 nm. Each composition of the solid solution is characterized by its unique absorption spectrum. Since all the NPs absorb visible light, they can be used as a photosensitive material for detection in the visible spectral range.

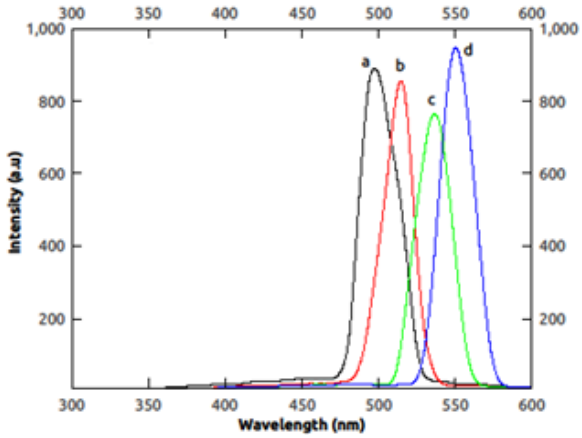

Fig. 6. Emission spectra of $Cu_xCd_{1-x}S$ (x = 0.8, 0.6, 0.4, 0.2) NPs: $Cu_{0.8}Cd_{0.2}S$ (a), $Cu_{0.6}Cd_{0.4}S$ (b), $Cu_{0.4}Cd_{0.6}S$ (c), $Cu_{0.2}Cd_{0.8}S$ (d).

3.3.2. PL studies

Fig. 6 illustrates the photoluminescence spectra of the as-synthesized $Cu_xCd_{1-x}S$ (x = 0.8, 0.6, 0.4, and 0.2) NPs. As can be seen from this figure, the emission peaks are found at 497, 515, 532, and 550 nm. With the increase in the Cd content, the emission spectrum shifts from that of pure CuS [28] to the one of pure CdS [29]. Fig. 7 shows the dependence of the emission peak on the Cu content in the $Cu_xCd_{1-x}S$ (x = 0.8, 0.6, 0.4, and 0.2) NPs. Since this dependence is linear, the composition of $Cu_xCd_{1-x}S$ NPs can be tuned for emission at different wavelengths in the range of 497…550 nm. Reversely, the sample composition can be identified by its emission peak.

4. Conclusions

In this work, $Cu_xCd_{1-x}S$ (x = 0.8, 0.6, 0.4, and 0.2) NPs were synthesized by microwave-assisted chemical precipitation method. The prepared samples were characterized by XRD, SEM, EDAX, UV-VIS, and PL spectroscopy. Presence of such elements as copper, cadmium, and sulphur was confirmed by the EDAX analysis. All the samples underwent phase transition above a certain temperature. By replacing 20% of Cu by Cd in the $Cu_{0.8}Cd_{0.2}S$ NPs, the resistance at room temperature could be changed from ~10^3 to ~10^5 Ohm. Each $Cu_xCd_{1-x}S$ composition was characterized by its unique absorption spectrum. Since the emission peak wavelength linearly depends on the Cu content in the $Cu_xCd_{1-x}S$ (x = 0.8, 0.6, 0.4, and 0.2) NPs, these NPs may be tuned to emit at different wavelengths in the range of 497…550 nm, and the sample composition can be identified by its emission peak.

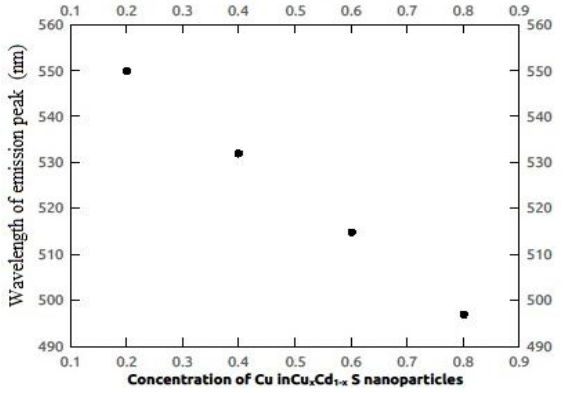

Fig. 7. Emission peak wavelength *vs* Cu content in $Cu_xCd_{1-x}S$ (x = 0.8, 0.6, 0.4, and 0.2) NPs.

Acknowledgements

The authors gratefully acknowledge Nesamony Memorial Christian College, Marthandam, for providing the necessary laboratory facilities to carry out this work.

Disclosure statement

No potential conflict of interest was reported by the authors.

Funding

This study was carried out as a part of the Ph.D. work of Mrs. Moly M. Rose and was not funded by any external agencies.

Data availability statement

The data that support the findings of this study are available within the article.

References

1. Selvi S.S.T., Linet J.M., Sagadevan S. Influence of CTAB surfactant on structural and optical properties of CuS and CdS nanoparticles by hydrothermal route. *J. Exp. Nanosci.* 2018. **13**, No 1. P. 130–143. https://doi.org/10.1080/17458080.2018.1445306.
2. Offiaha S.U., Ugwokea P.E., Ekwealorb A.B.C. *et al*. Structural and spectral analysis of chemical bath deposited copper sulphide thin film for solar energy conversions. *Dig. J. Nanomater. Bios.* 2012. **7**, No 1. P. 165–173.
3. Ghribi F., Alyamani A., BenAyadi Z. *et al*. Study of CuS thin films for solar cell applications sputtered from nanoparticles synthesised by hydrothermal route. *Energy Procedia*. 2015. **84**. P. 197–203. https://doi.org/10.1016/j.egypro.2015.12.314.
4. Wang H., Sun Y., Yue W. *et al*. A smartphone-based double-channel fluorescence setup for immunoassay of a carcinoembryonic antigen using CuS nanoparticles for signal amplification. *Analyst*. 2018. **143**. P. 1670–1678. https://doi.org/10.1039/C7AN01988B.
5. Ravele M.P., Oyewo O.A. Onwudiwe D.C. Controlled synthesis of CuS and Cu_9S_5 and their application in the photocatalytic mineralization of tetracycline. *Catalysts*. 2021. **11**. P. 899. https://doi.org/10.3390/catal11080899.
6. Ayodhya D., Veerabhadram G. Investigation of temperature and frequency dependence of electrical conductivity and dielectric behavior in CuS and rGO capped CuS nanocomposites. *Mater. Res. Express*. 2019. **6**. P. 045910. https://doi.org/10.1088/2053-1591/aafe55.
7. Zha Z., Zhang S., Deng Z. *et al*. Enzyme-responsive copper sulphide nanoparticles for combined photo-acoustic imaging, tumor-selective chemotherapy and photothermal therapy. *Chem. Commun*. 2013. **49**, No 33. P. 3455–3457. https://doi.org/10.1039/c3cc40608c.
8. Goel S., Chen F., Cai W. Synthesis and biomedical applications of copper sulfide nanoparticles: From sensors to theranostics. *Small*. 2014. **10**, No 4. P. 631–645. https://doi.org/10.1002/smll.201301174.
9. Gao W., Sun Y., *et al.* Copper sulfide nanoparticles as a photothermal switch for TRPV1 signaling to attenuate atherosclerosis. *Nature Commun*. 2018. **9**, No 1. https://doi.org/10.1038/s41467-017-02657-z.
10. Pal M., Mathews N.R., Santiago P., Mathew X. A facile one-pot synthesis of highly luminescent CdS nanoparticles using thioglycerol as capping agent. *J. Nanopart. Res.* 2012. **14**. P. 916. https://doi.org/10.1007/s11051-012-0916-3.
11. Martınez-Alonso C., Cortina-Marrero H.J., Coria-Monroy C.S. *et al*. Solution synthesized CdS nanoparticles for hybrid solar cell applications. *J. Mater. Sci.: Mater. Electron*. 2015. **26**. P. 5539–5545. https://doi.org/10.1007/s10854-014-2072-2.
12. Kowshik M., Deshmukh N., Vogel W. *et al*. Microbial synthesis of semiconductor CdS nanoparticles, their characterization, and their use in the fabrication of an ideal diode. *Biotechnol. Bioeng*. 2002. **78**, No 5. P. 583–588. https://doi.org/10.1002/bit.10233.
13. Ayodhya D., Venkatsham M., Santhoshi Kumari A. *et al*. One-spot sonochemical synthesis of CdS nanoparticles: Photocatalytic and electrical properties. *Int. J. Ind. Chem*. 2015. **6**. P. 261–271. https://doi.org/10.1007/s40090-015-0047-7.
14. Ma R.-M., Dai L., Huo H.-B. *et al.* High-performance logic circuits constructed on single CdS nanowires. *Nano Lett.* 2007. **7**, No 11. P. 3300–3304. https://doi.org/10.1021/nl0715286.
15. Duan X., Huang Y., Agarwal R., Lieber C.M. Single-nanowire electrically driven lasers. *Nature*. 2003. **421**. P. 241–245. https://doi.org/10.1038/nature01353.
16. Prokopenko S.L., Gunja G.M. *et al*. Synthesis and electrophysical properties of composite materials based on heterostructures CuS/CdS, Cu_2S/CdS, Ag_2S/CdS. *J. Nanostruct. Chem.* 2014. **4**. P. 103–108. https://doi.org/10.1007/s40097-014-0120-3.
17. Kim M., Altantuya U., Lee H. CuS/CdS quantum dot composite sensitizer and its applications to various TiO_2 mesoporous film-based solar cell devices. *Langmuir*. 2015. **31**, No 27. https://doi.org/10.1021/acs.langmuir.5b00324.
18. Yang X., Lu G., Wang B. *et al*. Synthesis, growth mechanism and photocatalytic H_2 evolution of CdS/CuS composite *via* hydrothermal method. *RSC Adv*. 2019. **9**. P. 25142–25150. https://doi.org/10.1039/C9RA04336E.
19. Li Z.G., Zeng B. CdS nanoparticle-decorated CuS microflower-2D graphene hybrids and their enhanced photocatalytic performance. *Chalcogenide Lett*. 2021. **18**, No 1. P. 39–46.
20. Steimle B.C., Lord R.W., Schaak R.E. Induced phase transition in copper sulfide nanoparticles prior to initiation of a cation exchange reaction. *J. Am. Chem. Soc*. 2020. **142**. P. 13345−13349. https://doi.org/10.1021/jacs.0c06602.
21. Rose M.M., Christy R.S. *et al.* Phase transitions in cadmium sulfide nanoparticles. *AIP Adv*. 2021. **11**. P. 085129. https://doi.org/10.1063/5.0052078.
22. Christy R.S., Kumaran J.T.T. Phase transition in CuS nanoparticles. *J. Non-Oxide Glasses.* 2014. **6**, No 1. P. 13–22.

23. Rose M.M., Christy R.S., Benitta T.A. *et al.* Phase transition in ZnS nanoparticles: electrical, thermal, structural, optical, morphological, antibacterial and photocatalytic properties. *Chalcogenide Lett*. 2022. **19**, No 11. P. 855–869.
24. Christy R.S., Kumaran J.T. Thanka *et al.* Phase transition in CuS-Ag_2S nanoparticle system. Phase transition. 2015. **89**. P. 155–166. http://doi.org/10.1080/01411594.2015.1102257.
25. Panda B.B., Sharma B., Rana R.K. Ultrasound mediated synthesis of CuS nanocrystallites. *Materials Science – Poland*. 2016. **34**, No 2. P. 446–450. https://doi.org/10.1515/msp-2016-0062.
26. Li Y., Lu W., Huang Q. *et al.* Copper sulfide nanoparticles for photothermal ablation of tumor cells. *Nanomedicine*. 2010. **5**, No 8. P. 1161–1171. https://doi.org/10.2217/nnm.10.85.
27. Ayodhya D., Veerabhadram G. Preparation, characterization, photocatalytic, sensing and antimicrobial studies of *Calotropis gigantea* leaf extract capped CuS NPs by a green approach. *J. Inorg. Organomet. Polym. Mater.* 2017. **27**, S1. P. 215–230. doi.org/10.1007/s10904-017-0672-z.
28. Yadav S. Bajpai P.K. Synthesis of copper sulfide nanoparticles: pH dependent phase stabilization. *Nano-Structures & Nano-Objects.* 2017. **10**. P. 151–158. https://doi.org/10.1016/j.nanoso.2017.03.009.
29. Mohsennia M., Bidgoli M.M., Boroumand F.A. Low driving voltage in polymer light-emitting diodes with CdS nanoparticles as an electron transport layer. *J. Nanophoton*. 2015. **9**, No 1. P. 093081. https://doi.org/10.1117/1.jnp.9.093081.

Authors and CV

Dr. Moly M. Rose, born in 1983, Assistant Professor at the Mar Ephraem College of Engineering and Technology. She defended her Ph.D. thesis in Physics in 2024 at the Nesamony Memorial Christian College Marthandam. Authored over 5 publications. The area of her scientific interests includes physics and technology of semiconductor materials, hetero- and hybrid structures, and devices.
https://orcid.org/0000-0003-4840-0567

Dr. R. Sheela Christy, born in 1969, Associate Professor at the Nesamny Christian College Marthandam. She defended her Ph.D. thesis in Physics in 2016 at the same college. Authored over 20 publications. The area of her scientific interests includes physics and technology of nanosized semiconductor materials.
E-mail: sheelachristy@gmail.com

Dr. T. Asenath Benitta, born in 1986, Assistant Professor at the Nesamny Christian College Marthandam. She defended her Ph.D. thesis in Physics in 2018 at the same college. Authored over 9 publications. The area of her scientific interests includes physics, surface enhanced Raman spectroscopy, and nanotechnology.
E-mail: asenathbenitta@gmail.com

Dr. J. Thampi Thanka Kumaran, born in 1958, Principal of Malankara Catholic College (Retired). He defended his Ph.D. thesis in Physics in 1998 at the Nesamony Memorial Christian College Marthandam. Authored over 25 publications. The area of his scientific interests includes physics, surface enhanced Raman spectroscopy, and nanotechnology.
E-mail: thampithankakumaran@gmail.com

Authors' contributions

Rose M.M.: investigation, writing – review & editing.
Christy R.S.: investigation, writing – review & editing.
Benitta T.A.: investigation, writing – review & editing.
Kumaran J.T.T.: conceptualization, methodology, formal analysis, data curation, writing – original draft, visualization, writing – review & editing.

All the authors discussed the results and contributed to the final manuscript.

Фазовий перехід та порівняльне дослідження системи наночастинок $Cu_xCd_{1-x}S$ (x = 0.8, 0.6, 0.4 та 0.2)

M.M. Rose, R.S. Christy, T.A. Benitta, J.T.T. Kumaran

Анотація. Суміш наночастинок $Cu_xCd_{1-x}S$ (x = 0.84, 0.6, 0.4 та 0.2) отримано хімічним осадженням під дією мікрохвильового випромінювання. Кристалічну структуру, розмір і морфологію поверхні синтезованих наночастинок було досліджено методами дифракції рентгенівських променів та скануючої електронної мікроскопії. Наявність у зразках міді, кадмію та сірки в належних співвідношеннях було підтверджено енергодисперсним рентгенівським аналізом. Вимірювання електричного опору при постійному струмі у діапазоні температур 300…500 K продемонстрували, що у всіх зразках відбувається фазовий перехід при температурі, вищій за певну температуру.

Ключові слова: наночастинки, хімічне осадження, фазовий перехід, ширина забороненої зони, електричний опір.